Z. Phys. C – Particles and Fields 40, 163–170 (1988)

Zeitschrift für Physik C Particles and Fields

A measurement of muon pair production in e^+e^- annihilation at centre of mass energies $35.0 \leqq \sqrt{s} \leqq 46.8$ GeV

TASSO Collaboration

W. Braunschweig, R. Gerhards, F.J. Kirschfink, H.-U. Martyn
I. Physikalisches Institut der RWTH Aachen, D-5100 Aachen, Federal Republic of Germany[a]

B. Bock[1], H.M. Fischer, H. Hartmann, J. Hartmann, E. Hilger, A. Jocksch, R. Wedemeyer
Physikalisches Institut der Universität Bonn, D-5300 Bonn, Federal Republic of Germany[a]

B. Foster, A.J. Martin, A.J. Sephton
H.H. Wills Physics Laboratory, University of Bristol, Bristol BS8 1TL, UK[b]

E. Bernardi, J. Chwastowski[2], A. Eskreys[3], K. Gather, K. Genser[4], H. Hultschig, P. Joos, H. Kowalski, A. Ladage, B. Löhr, D. Lüke, P. Mättig[5], D. Notz, J.M. Pawlak[6], K.-U. Pösnecker, E. Ros, D. Trines, R. Walczak[4], G. Wolf
Deutsches Elektronen-Synchrotron, DESY, D-2000 Hamburg, Federal Republik of Germany

H. Kolanoski
Institut für Physik, Universität Dortmund, D-4600 Dortmund, Federal Republic of Germany[a]

T. Kracht[7], J. Krüger, E. Lohrmann, G. Poelz, W. Zeuner
II. Institut für Experimentalphysik der Universität Hamburg, D-2000 Hamburg, Federal Republic of Germany[a]

J. Hassard, J. Shulman, D. Su
Department of Physics, Imperial College, London SW7 2AZ, UK[b]

F. Barreiro, L. Hervas, A. Leites, J. del Peso, M. Traseira
Universidad Autónoma de Madrid, E-28049 Madrid, Spain[c]

C. Balkwill, M.G. Bowler. P.N. Burrows, R.J. Cashmore, C.M. Hawkes[8], G.P. Heath, P.N. Ratoff, I.M. Silvester, I.R. Tomalin, M.E. Veitch
Department of Nuclear Physics, Oxford University, Oxford OX1 3RH, UK[b]

G.E. Forden[9], J.C. Hart, D.H. Saxon
Rutherford Appleton Laboratory, Chilton, Didcot, Oxon OX11 0QX, UK[b]

S. Brandt, M. Holder, L. Labarga[10]
Fachbereich Physik der Universität-Gesamthochschule Siegen, D-5900 Siegen, Federal Republic of Germany[a]

E. Duchovni, Y. Eisenberg, U. Karshon, G. Mikenberg, A. Montag, D. Revel, E. Ronat, A.N. Wainer, G. Yekutieli
Weizmann Institute, Rehovot 76100, Israel[d]

D. Muller, S. Ritz, D. Strom[11], M. Takashima, Sau Lan Wu, G. Zobernig
Department of Physics, University of Wisconsin, Madison, WI 53706, USA[e]

Received 6 May 1988

[1] Now at Krupp Atlas Elektr. GmbH, Bremen FRG
[2] On leave from Inst. of Nuclear Physics, Cracow, Poland
[3] Now at Inst. of Nuclear Physics, Cracow, Poland
[4] Now at Warsaw University, Poland
[5] Now at IPP Canada, Carleton University, Ottawa, Canada
[6] On leave from Warsaw University, Poland
[7] Now at Hasylab, DESY, Hamburg, FRG
[8] Now at California Institute of Technology, Pasadena, CA, USA
[9] Now at SUNY Stony Brook, Stony Brook, NY, USA
[10] Now at SLAC, Stanford, CA, USA
[11] Now at University of Chicago, Chicago, IL. USA

[a] Supported by the Bundesministerium für Forschung und Technologie
[b] Supported by the UK Science and Engineering Research Council
[c] Supported by CAICYT
[d] Supported by the Minerva Gesellschaft für Forschung mbH
[e] Supported by the US Dept. of Energy, contract DE-AC02-76ER0088 by the U.S. National Science Foundation Grant no. INT-8313994 for travel
[f] Partially supported by grant CPBP 01.06

Abstract. The reaction $e^+e^- \to \mu^+\mu^-$ has been studied at centre of mass energies between 35.0 and 46.8 GeV using the TASSO detector at PETRA. We present measurements of the forward-backward charge asymmetry ($A_{\mu\mu}$) and cross section ($\sigma^{\mu\mu}$) for this reaction at three energies. At 35.0 GeV we obtain a cross section relative to the QED prediction of $R_{\mu\mu} = (\sigma^{\mu\mu}/\sigma^0) = 0.932 \pm 0.018 \pm 0.044$ and $A_{\mu\mu} = (-10.6^{+2.2}_{-2.3} \pm 0.5)\%$. At 38.3 GeV we find $R_{\mu\mu} = 0.951 \pm 0.072^{+0.063}_{-0.057}$ and $A_{\mu\mu} = (+1.7^{+8.5}_{-8.6} \pm 0.5)\%$. At 43.6 GeV we measure $R_{\mu\mu} = 0.921 \pm 0.037 \pm 0.055$ and $A_{\mu\mu} = (-17.6^{+4.4}_{-4.3} \pm 0.5)\%$. Our results are in good agreement with the predictions of the standard model. Including previous TASSO data we present improved determinations of muonic electroweak parameters. We also report on lower limits of possible contributions from contact interactions.

1 Introduction

The standard model [1], based on the gauge group $SU(3) \times SU(2)_L \times U(1)$, accounts for many phenomena in high energy physics. There remain, however, many features of the model which have yet to be examined and it is important to use as diverse a range of experiments as possible to test the standard model.

The reaction $e^+e^- \to \mu^+\mu^-$ probes the electroweak sector of the standard model without the complication, at lowest order, of the presence of strong interactions. The electroweak interference between vector and axial-vector currents leads to a forward-backward asymmetry in the angular distribution of the muons. This asymmetry is sensitive to the effects of the Z° pole in the range of energies which have been explored at PETRA, its magnitude significantly increasing with energy.

In this paper we report on the results of an analysis of the reaction $e^+e^- \to \mu^+\mu^-$ at $\sqrt{s} = 35.0$ GeV, 38.3 GeV and up to 46.8 GeV, the highest energies reached at PETRA. The data were accumulated with the TASSO detector during three years of high energy operation of the PETRA storage ring between 1983 and 1985 followed by a year of high luminosity running at 35.0 GeV. A total integrated luminosity of 44.0 pb^{-1} was collected at centre of mass energies in excess of 38 GeV (mostly at 38.3 GeV and 43.6 GeV) and 108.5 pb^{-1} at 35.0 GeV.

2 Event selection

The experimental apparatus and the trigger have been described previously [2]. In this paper we use similar analysis methods and more details can be found in the above references, the appendix and [3, 4]. The selection criteria are described in detail in the appendix and were chosen a) to reject cosmic ray events using the inner time of flight (ITOF) counters and the proximity of the event vertex to the intersection region and b) to reject two-photon scattering ($\gamma\gamma$) events and tau pair events by requiring that both charged tracks had more than half of the beam momentum and that the acollinearity angle between the muon tracks was less than 10°. Finally, after application of a solid angle cut, the events were required to have at least one muon identified with the muon chambers or the liquid argon barrel calorimeter (LABC). It should be noted that the only changes to the selection cuts described in [2] were: a) low momentum tracks not originating near the intersection region, or which were badly reconstructed, were ignored before requiring exactly two tracks in the event (this avoids the loss of good muon pair events which would otherwise be rejected due to the presence of extra tracks from converting bremsstrahlung photons, stray off-momentum beam particles and spurious tracks) and b) the criteria for identifying a track as a muon in the LABC were changed for the 35.0 GeV data, due to different operating conditions during the 1986 running period.

The selected events were scanned to remove the few remaining Bhabha scattering events which had survived the previous cuts as a result of false identification of one track in the LABC. This occurred when the electron shower cluster had been split and the track had been associated with a low energy fragment which was consistent with the deposit from a minimum ionizing particle. Only unambiguous Bhabha events were rejected, and tau pair events containing one good muon track were kept since these are accounted for in the background subtraction.

The final data sets contain 612 events at $\sqrt{\langle s \rangle} = 43.6$ GeV, 173 events at $\sqrt{s} = 38.3$ GeV and 2563 events at $\sqrt{s} = 35.0$ GeV.

3 Measurement of efficiencies

The efficiencies for triggering, muon identification and selection of muon pair candidates were calculated using the muon pair data, the hadronic data and a sample of Bhabha scattering events.

3.1 Trigger efficiency

Muon pair events were required to set the coplanar trigger [2] which underwent several changes during the data taking period. The essential requirement throughout was that there be at least two back-to-back charged tracks. The degree to which the two tracks had to be collinear was changed depending on the conditions of data taking. For most of the 35.0 GeV data and some of the high energy data the requirement was that the tracks be collinear to within 27° in the plane perpendicular to the beam axis, whereas for the rest of the data the cut was at 13°, to reduce the number of triggers due to noise. A charged track candidate was identified at the trigger level by requiring connected information in the inner tracking chambers, associated with a hit in one of the 48 inner time of flight scintillator counters.

In our previous analysis [2] the efficiency was measured using Bhabha scattering events which had set independent calorimeter triggers (based on the LABC or hadron arm shower counters) since there was no independent trigger selecting muon pair events. Assuming that the coplanar trigger efficiency for muon pairs was the same as for Bhabhas these events were then used to measure the probability that the coplanar trigger was set.

In this analysis we have measured the efficiency for producing connected tracks in the tracking chamber system using a sample of Bhabha scattering events selected with calorimeter triggers. The difference in this efficiency for muon pairs and Bhabhas was estimated to be less than 2%. The efficiency for setting the ITOF counters was measured using isolated tracks in hadronic events. Small corrections were made for photons converting and setting the ITOF counters, pions undergoing nuclear interactions and also for noise in the counters.

The efficiencies varied throughout the course of the data taking, but the overall trigger efficiency was typically between 77% and 88% [3, 4].

3.2 Selection efficiency

The efficiency with which muon pair events were selected from the raw data tapes using the cuts described in the appendix was also determined using the sample of Bhabhas obtained with independent calorimeter triggers. The fraction of these events which passed all the muon pair selection cuts apart from the muon identification criteria gave the event selection efficiency. This varied slightly between 95% and 96% in different run periods.

3.3 Identification efficiency

The efficiency of the muon identification criteria was calculated in a variety of different ways, which gave consistent results. Since only one track was required to be identified as a muon in each event, the opposite tracks (if they also entered the acceptance of the detector) could be used as an independent unbiassed sample of muon tracks from which to calculate the muon identification efficiency of the detector. Allowance must be made for the small background of tau pair events in the final sample in which only one of the two tracks was a genuine muon. For tracks which entered the common acceptance of the muon chambers and the LABC, those tracks identified as muons by one detector system were used as an unbiassed sample of muon tracks to calculate the muon identification efficiency of the other system. Again allowance must be made for the small background of tau pair events in the final sample in which minimum ionizing hadronic tracks may be wrongly identified as muons in the LABC, but will not be identified as muons in the muon chambers. The efficiency has also been calculated using cosmic ray events in which we can look separately at each track without requiring identification of either track and hence can look for correlated inefficiencies between the different chambers. Inside the region of acceptance of the muon chambers and LABC the overall efficiency for identifying one track or more in a muon pair event as a muon was in excess of 99% for the muon chambers and in the range 89% to 95% for the LABC.

The probability of misidentifying the charge of tracks in Bhabha events has been shown to be very low in the TASSO detector [5], $0.3 \pm 0.1\%$ $(0.5 \pm 0.1)\%$ at $\sqrt{s} = 35$ GeV (44 GeV) and a correlated probability that both tracks have their charges wrongly assigned of less than 10^{-5} (2×10^{-5}) at $\sqrt{s} = 35$ GeV (44 GeV). This is consistent with the assumption that both curvature measurements are independent of each other. Muon pairs identified with the same charge were used for the total cross-section measurement but not in the asymmetry measurement. The possibility of a forward-backward bias in the data has also been ruled out [2].

3.4 Geometrical acceptance calculation

The geometrical acceptance of the TASSO detector for muon pairs was calculated using Monte Carlo techniques [6]. Events were generated with the correct beam energies from each run period and weighted by the appropriate integrated luminosities. The acceptance is defined as the number of events generated and passing all muon pair selection criteria to the number of events generated and satisfying the momentum and acollinearity cuts. The total combined acceptance, found by integrating over the solid angle $(-0.8 \leq \cos\bar{\theta} \leq 0.8)$, varied between 64% and 71%. $(\cos\bar{\theta} = \mathbf{e}^+ \cdot (\boldsymbol{\mu}^+ - \boldsymbol{\mu}^-)/|\mathbf{e}^+| |(\boldsymbol{\mu}^+ - \boldsymbol{\mu}^-)|$, where $\mathbf{e}^+$ is the momentum vector of the positron etc.)

4 Backgrounds

The cuts described above were designed to remove background due to tau pairs, cosmic rays, Bhabha scattering events and $e^+e^- \to e^+e^-\mu^+\mu^-$ events. The remaining background from these sources was calculated using either Monte Carlo techniques or the data directly. The background from the last three processes was found to be negligible.

The main background was from tau pair events in which each tau decays to one charged track, at least one of which was identified as a muon. This background was estimated by generating Monte Carlo $\tau^+\tau^-$ events to which were applied the muon pair selection cuts and was found to be 3–5% in each of our muon data sets, but with a large uncertainty ($\sim\pm 2\%$) due to uncertainties in the simulation of hadrons in the LABC. The $\tau^+\tau^-$ background was statistically subtracted from the final data sets before calculating the $e^+e^-\to\mu^+\mu^-$ cross-section.

5 Systematic errors

The combined systematic error on the total cross section varied between 4.7 and 6.6%. The major contributions to this were from the uncertainty in the luminosity (3.0–3.6%), the uncertainty in the trigger efficiency (3.2–4.4%) and the uncertainty in the background subtraction (1.5–2.3%). Other sources of systematic error such as uncertainty in the muon identification efficiencies, the Monte Carlo simulation, and the selection efficiency all gave much smaller contributions.

The systematic error on the asymmetry is of course much smaller than the systematic error on the total cross section, as most of the uncertainties cancel out. A detailed check of the symmetry of the apparatus and analysis procedure has been carried out previously [10]. No evidence for any artificially introduced asymmetry could be detected and the resulting absolute systematic uncertainty on the asymmetry was estimated to be $\pm 0.5\%$.

6 Radiative corrections

The measured total cross section depends on the experimental cuts since they control the contributions of bremsstrahlung diagrams producing $\mu^+\mu^-\gamma$ final states with non-zero acollinearity angle. The radiative correction function is calculated to correct the measured differential cross-section to correspond to the lowest order cross section and is a function of $\cos\bar{\theta}$ as well as the momentum and acollinearity angle cuts. A more complete discussion of the problems involved in calculating and implementing the radiative corrections may be found in [3, 6–9]. One problem with publishing asymmetries after radiative corrections have been applied, is that if new calculations are performed, then it becomes necessary to undo the original radiative corrections in order to use the new calculations. It has therefore been suggested [3, 7] that results should also be published before any radiative corrections have been performed. We present our differential cross section and asymmetry results with 'reduced QED' radiative corrections and also quote, for convenience, numbers for the asymmetry measurements without any radiative corrections.

The radiative correction function was calculated using Monte Carlo techniques [6] using all purely electromagnetic contributions at order α^3 (known as 'reduced QED' corrections in the literature). Order α^3 weak corrections to both photon- and Z^0-exchange diagrams were not included, as the small contributions from these diagrams almost cancel out the small contributions from the order α^3 electromagnetic corrections to Z^0-exchange diagrams, which were also omitted [8]. For example for the TASSO acceptance at $\sqrt{s}=44$ GeV the lowest order electroweak interference contribution to the forward-backward muon pair asymmetry is calculated to be -13.6% compared with contributions of $+1.8\%$ from purely electromagnetic diagrams, $+1.0\%$ from the electromagnetic corrections to Z^0-exchange diagrams and -1.1% from weak corrections to the photon- and Z^0-exchange diagrams [8]. However given the statistical precision of the data the size of these higher order terms cannot be tested quantitatively.

7 Results

The total cross section results for the three data sets described in this paper are given in Table 1 together with those from our earlier publication [2]. We define $R_{\mu\mu}$ as $\sigma^{\mu\mu}/\sigma^0$ where $\sigma^{\mu\mu}$ is the measured muon pair cross section after 'reduced QED' radiative corrections have been applied and σ^0 is the lowest order QED prediction. At PETRA energies the effect of Z^0 exchange on the total cross section is very small, and $R_{\mu\mu}$ is predicted to be very close to 1. Even at $\sqrt{s}=43.6$ GeV the expected deviation from QED is only about 1%. The results for $\sigma^{\mu\mu}$ are shown in Fig. 1

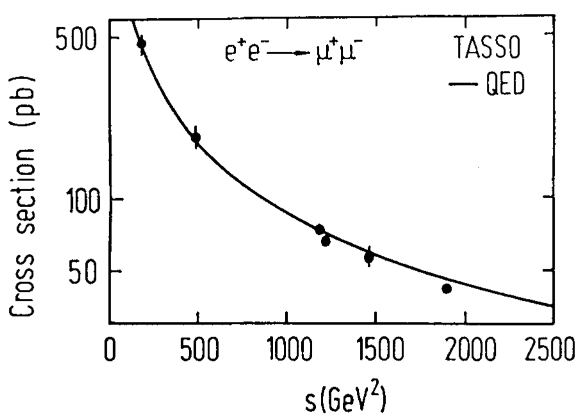

Fig. 1. The total cross section for the reaction $e^+e^-\to\mu^+\mu^-$ as a function of s. The curve shows the QED prediction. Statistical errors only are shown

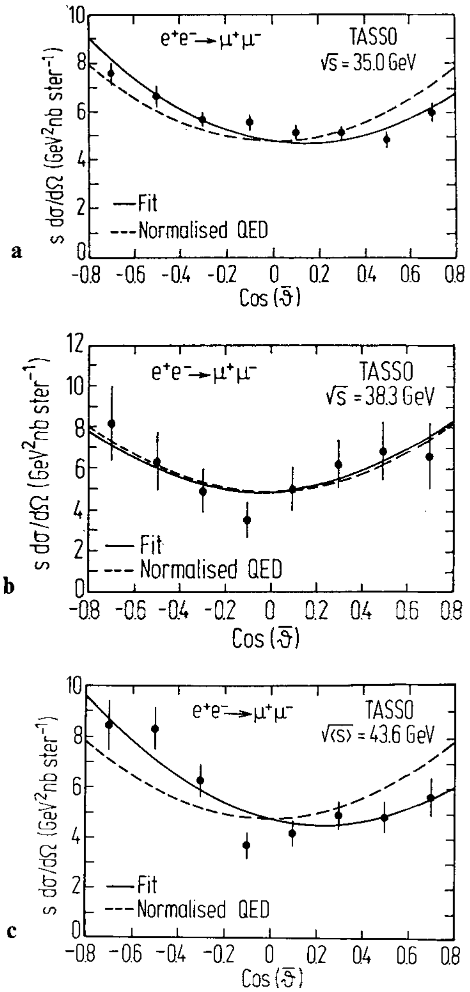

Fig. 2a–c. The differential cross section $s \cdot \frac{d\sigma}{d\Omega}$ for the reaction $e^+e^- \to \mu^+\mu^-$ at energies of **a** $\sqrt{s}=35.0$ GeV, **b** $\sqrt{s}=38.3$ GeV and **c** $\sqrt{\langle s\rangle}=43.6$ GeV. 'Reduced QED' corrections have been applied. The solid line shows the result of a fit to the standard model, the dashed line is the prediction of QED normalised to the observed total cross section. Statistical errors only are shown

together with previous TASSO data at lower energies. The new cross section measurements fall slightly below the QED predictions (solid curve), however, this difference is not inconsistent with the systematic uncertainties.

In the standard model [1] the lowest order differential cross section for $e^+e^- \to \mu^+\mu^-$ is given by

$$\frac{d\sigma}{d\Omega}=\frac{\alpha^2}{4s}(C_1(1+\cos^2\theta)+C_2\cos\theta)$$

where

$$C_1=1+2g_V^e\, g_V^\mu\, \mathrm{Re}(\chi)+(g_V^{e2}+g_A^{e2})(g_V^{\mu 2}+g_A^{\mu 2})|\chi|^2$$

and

$$C_2=4g_A^e\, g_A^\mu\, \mathrm{Re}(\chi)+8g_V^e\, g_V^\mu\, g_A^e\, g_A^\mu |\chi|^2.$$

$g_V^e, g_V^\mu, g_A^e, g_A^\mu$ are the vector and axial vector couplings of the electron and muon. In the standard model

$$g_A^e=g_A^\mu=-1/2 \quad \text{and} \quad g_V^e=g_V^\mu=-1/2+2\sin^2\theta_w.$$

The function χ is given by the neutral current coupling, i.e. the weak mixing angle, $\sin^2\theta_w$, and the Z^0 propagator and has been parametrised as follows [11]:

$$\chi=\frac{1}{4\sin^2\theta_w\cos^2\theta_w}\,\frac{s}{s-M_Z^2+iM_Z\Gamma_Z}.$$

The advantage of this scheme is that electroweak one-loop corrections are small [8] and hence it is valid to compare the predicted asymmetry using this parametrisation with the measured asymmetry to which only 'reduced QED' corrections have been applied.

The forward-backward asymmetry in the differential cross-section extrapolated over the full angular range is given by

$$A_{\mu\mu}=\frac{3}{8}\cdot\frac{C_2}{C_1}\simeq\frac{3}{2}g_A^e\, g_A^\mu\, \mathrm{Re}(\chi).$$

For all numerical calculations within the standard model we use $\sin^2\theta_w=0.226\pm0.007$, $M_Z=(91.9 \pm 1.8)$ GeV [12] and $\Gamma_Z=3$ GeV.

The differential cross sections at $\sqrt{s}=35.0$ GeV, $\sqrt{s}=38.3$ GeV and $\sqrt{\langle s\rangle}=43.6$ GeV are shown in Figs. 2a–c ('reduced QED' radiative corrections were applied and only statistical errors are shown) and listed in Table 2. A maximum likelihood fit gives the asymmetries extrapolated to the full polar range given in Table 1.

The data at 35.0 GeV and 43.6 GeV show a clear

Table 1. Data samples and results of total cross section and asymmetry measurements of the reaction $e^+e^- \to \mu^+\mu^-$. When two errors are given, the first is statistical and the second systematic, when only one is given this is the sum of the two in quadrature

$\sqrt{s}$ (GeV)	Luminosity (pb^{-1})	Number of events	$\sigma^{\mu\mu}$ (pb)	$R_{\mu\mu}$	$A_{\mu\mu}$	A_{GWS}
13.9	1.7	341	472.7 ± 36.0	1.05 ± 0.08	$(-1\pm6)\%$	-1.2%
22.3	3.2	268	184.7 ± 15.7	1.06 ± 0.09	$(-13\pm7)\%$	-3.3%
34.5	74.7	2673	$73.2\pm1.5\pm2.6$	$1.002\pm0.020\pm0.035$	$(-9.1\pm2.3\pm0.5)\%$	-8.6%
35.0	108.5	2563	$66.1\pm1.3\pm3.1$	$0.932\pm0.018\pm0.044$	$(-10.6^{+2.2}_{-2.3}\pm0.5)\%$	-8.9%
38.3	8.8	173	$56.4\pm4.4^{+3.7}_{-3.4}$	$0.951\pm0.072^{+0.063}_{-0.057}$	$(+1.7^{+8.5}_{-8.6}\pm0.5\%$	-11.0%
43.6	35.2	612	$42.0\pm1.7\pm2.5$	$0.921\pm0.037\pm0.055$	$(-17.6^{+4.4}_{-4.3}\pm0.5)\%$	-15.2%

Table 2. The differential cross sections, $s\frac{d\sigma}{d\Omega}$, for the reaction $e^+e^- \to \mu^+\mu^-$ at energies of 34.5, 35.0, 38.3 and 43.6 GeV. The data are corrected for 'reduced QED' radiative corrections. Statistical errors only are given. For the overall normalisation uncertainty see the text

$\cos\bar{\theta}$	Differential Cross Section Results $s\,d\sigma/d\Omega$(GeV^2 nb ster^{-1})			
	$\sqrt{\langle s\rangle}=34.5$ GeV	$\sqrt{s}=35.0$ GeV	$\sqrt{s}=38.3$ GeV	$\sqrt{\langle s\rangle}=43.6$ GeV
−0.8 – −0.6	7.12±0.43	7.59±0.46	8.23±1.85	8.45±0.96
−0.6 – −0.4	5.84±0.36	6.68±0.39	6.37±1.42	8.32±0.84
−0.4 – −0.2	5.46±0.30	5.73±0.30	4.94±1.08	6.28±0.64
−0.2 – 0.0	5.04±0.29	5.60±0.30	3.54±0.88	3.71±0.49
0.0 – 0.2	5.45±0.31	5.19±0.29	5.04±1.05	4.16±0.51
0.2 – 0.4	6.04±0.32	5.18±0.28	6.25±1.20	4.91±0.55
0.4 – 0.6	7.38±0.40	4.91±0.33	6.86±1.43	4.83±0.61
0.6 – 0.8	8.85±0.50	6.06±0.39	6.65±1.62	5.66±0.76

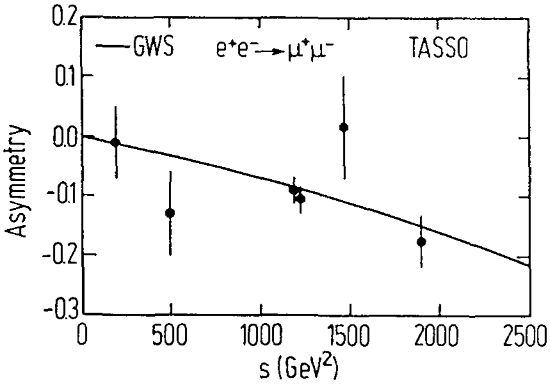

Fig. 3. The forward-backward muon pair asymmetry as a function of s. The solid line is the prediction of the standard model assuming $\sin^2\theta_w=0.226$ and $M_Z=91.9$ GeV

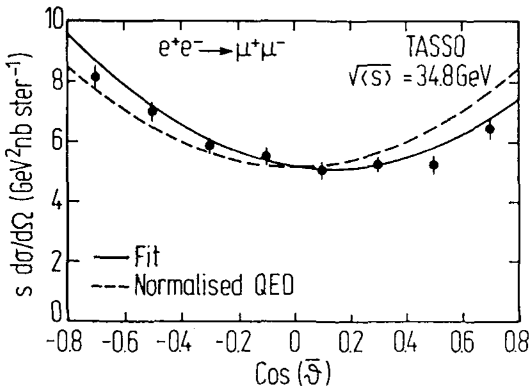

Fig. 4. The differential cross section $s\cdot\frac{d\sigma}{d\Omega}$ for the reaction $e^+e^- \to \mu^+\mu^-$ at $\sqrt{\langle s\rangle}=34.8$ GeV. 'Reduced QED' corrections have been applied. The solid line shows the result of a fit to the standard model, the dashed line is the prediction of QED normalised to the observed total cross section. Statistical errors only are shown

asymmetry, supporting the predictions of the standard model. The data at 38.3 GeV are statistically less significant. All TASSO results on muon pair asymmetries including previous measurements [2] covering the energy range $12<\sqrt{s}<47$ GeV are displayed in Fig. 3 and compiled in Table 1 together with the standard model predictions.

Following the recommendation of [3, 7] we have also calculated the asymmetries before applying radiative corrections, and have the following results $A_{\mu\mu}^{\text{norad}}=(-7.6\pm2.3\pm0.5)\%$, $(+4.9{+8.5 \atop -8.6}\pm0.5)\%$ and $(-15.2\pm4.3\pm0.5)\%$ at $\sqrt{s}=35.0$ GeV, 38.3 GeV and 43.6 GeV respectively.

For the remaining analysis we include our previous high statistics data at $\sqrt{s}=34.5$ GeV, the differential cross section is listed in Table 2 for convenience. They are in very good agreement with the new measurements at 35.0 GeV. The differential cross section of the combined data at an average energy of $\sqrt{\langle s\rangle}=34.8$ GeV is shown in Fig. 4. From a fit to the differential cross sections of all TASSO data the product of the axial vector couplings was found to be

$$g_A^e\cdot g_A^\mu=0.264\pm0.037.$$

Using $g_A^e=-0.498\pm0.027$ from neutrino electron scattering experiments [13] the axial vector coupling of the muon was determined to be $g_A^\mu=-0.530\pm0.080$. Alternatively, if the standard model weak isospin assignment of the leptons is assumed, the muon data can be used to check the consistency between otherwise determined values of $\sin^2\theta_w$ and M_Z [12]. Using the measured Z^0 mass we find

$$\sin^2\theta_w=0.191{+0.049+0.015 \atop -0.029-0.012},$$

where the second error is due to the uncertainty in the Z^0 mass. This value is consistent with the average value obtained from purely leptonic neutrino electron scattering [13]. Conversely, using $\sin^2 \theta_w$ and its error [13] as input the Z^0 mass is constrained by our muon data to be $M_Z = 93.1 \pm 2.5$ GeV.

8 Contact terms

It is conceivable that new physics beyond the standard model may occur at a scale Λ much beyond the present energy region. Such new phenomena could for example be substructures of the leptons or new currents, which may manifest themselves through their interference with the photon and Z^0 fields as residual contact interactions. The authors of [14] have proposed a general helicity conserving effective Lagrangian to be added to the standard model Lagrangian

$$L_{eff} = \pm \frac{g^2}{\Lambda_\pm^2}(\eta_{LL} j_L j_L + \eta_{RR} j_R j_R + 2\eta_{RL} j_R j_L).$$

The coupling constant is arbitrarily fixed to $g^2/4\pi = 1$, leaving the scale Λ as free parameter. j_L and j_R denote left-handed and right-handed currents. The coefficients η are restricted to the values 0 and ± 1, allowing four different helicity structures LL, RR, VV and AA to be constructed. The overall sign defines positive or negative interference.

All our high energy data above 30 GeV have been used to search for possible contributions of contact terms. Lower limits on the scale parameter Λ are summarised in Table 3. They range between 1.3 TeV and 3.5 TeV depending on the assumed chiral structure. LL and RR couplings are indistinguishable at present energies. The sensitivity of our highest statistics data at 34.8 GeV is illustrated in Fig. 5 for various values of Λ. Note that the traditional QED form factor is a special case of the vector type contact interaction. The respective cut-off parameters are related through $\Lambda^{QED} \simeq \sqrt{\alpha} \cdot \Lambda^{VV}$. We find lower limits (95% confidence level) of $\Lambda_+^{QED} > 325$ GeV and $\Lambda_-^{QED} > 150$ GeV.

Table 3. Lower limits (95% confidence level) on mass scale parameters Λ in contact interactions for left-handed (L), right-handed (R), vector (V), and axial vector (A) couplings from the reaction $e^+e^- \rightarrow \mu^+\mu^-$

Coupling	Λ_+ (TeV)	Λ_- (TeV)
LL	2.3	1.3
RR	2.3	1.3
VV	3.5	1.8
AA	3.2	2.9

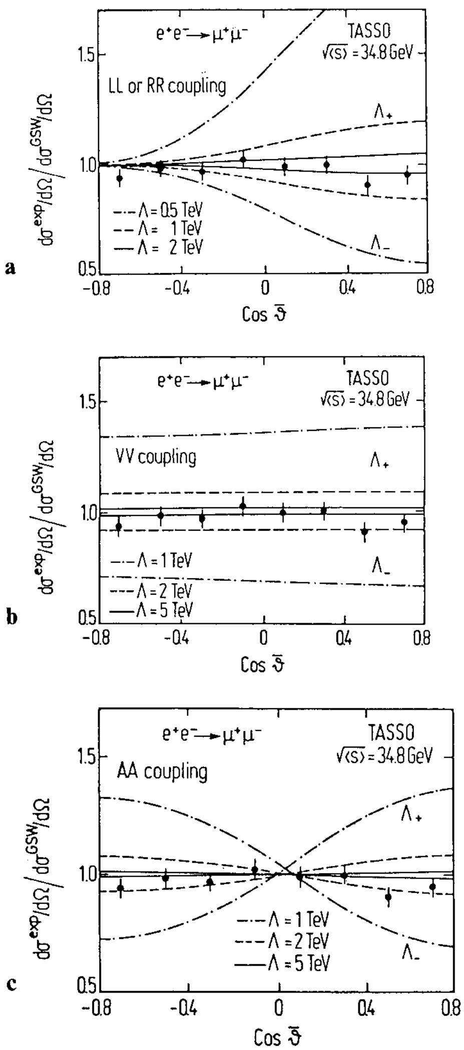

Fig. 5a–c. The differential cross section normalised to the prediction of the standard model for the reaction $e^+e^- \rightarrow \mu^+\mu^-$ at $\sqrt{\langle s \rangle} = 34.8$ GeV. The curves show possible contributions of contact terms for **a** left-handed or right-handed coupling, **b** vector coupling, and **c** axial vector coupling. Statistical errors only are shown

9 Summary

We have presented new measurements of the cross section and charge asymmetry for the reaction $e^+e^- \rightarrow \mu^+\mu^-$ at centre of mass energies between 35.0 and 46.8 GeV. Our results support the standard model predictions and are in good agreement with other experiments performed at these energies [15]. By including previous TASSO data we were able to improve the determination of leptonic electroweak coupling constants. We have reported on new lower limits on mass scale parameters of possible contributions of contact interactions.

Appendix

Selection criteria

In this section we give a summary of our selection criteria for the reaction $e^+e^- \rightarrow \mu^+\mu^-$. In order to simplify the description of these cuts we define the r-ϕ plane to be the plane perpendicular to the beams, which themselves define the z axis.

1. There must be exactly 2 tracks satisfying the following conditions:
   a) Momentum in $r-\phi$ plane >3 GeV/c.
   b) Vertex restriction
      (i) In the $r-\phi$ plane $|d_0|<15$ mm. (d_0 is the distance of the track from the origin in the $r-\phi$ projection at its point of closest approach.)
      (ii) In the z direction $|z_0|<75$ mm. (z_0 is the value of z at the point on the track from which d_0 is measured.)
   c) Reconstruction by our fitting program
      (i) χ^2/dof for fitting in $r-\phi<15$.
      (ii) χ^2/dof for fitting in $z<15$.

The remaining cuts were then applied considering only these 2 tracks.

2. Momentum of each track $P>P_{\text{beam}}/2$.
3. Acollinearity $\zeta<10°$, and acoplanarity $\psi<10°$ (ψ is the $r-\phi$ projection of ζ).
4. Timing cut -3.0 ns $<t_{\text{meas}}-t_{\text{pred}}<2.0$ ns for each track.
5. Tighter vertex restriction
   a) $|d_0^{\text{beam}}|<4$ mm. (d_0^{beam} is the distance in $r-\phi$ of the track from our best estimate of the beam position.)
   b) $|\langle z_0\rangle|<40$ mm. ($\langle z_0\rangle$ is the mean z_0 for the 2 tracks.)
6. Polar angle cuts
   a) Each of the tracks satisfied $|\cos\theta|<0.82$
   b) and $|\cos\bar{\theta}|<0.8$, where $|\cos\bar{\theta}|$ is defined in Sect. 3.4.
7. The coplanar trigger was set.
8. At least one of the tracks was identified as a muon in the muon chambers or LABC. In the muon chambers a particle was identified as a muon if the track penetrated the iron absorber and had associated hits in $\geqq 3$ out of the 4 muon chambers. In the LABC the criteria for identifying a particle as a muon were different for the 1986 35.0 GeV data and our other data sets due to deterioration in the performance of the calorimeter. For the 38.3 and 43.6 GeV data we required that the track deposit less than 1.5 GeV in a single cluster in the LABC, and also made cuts on the extent of the shower. For the 35.0 GeV data we tightened the cuts on the size of the shower and also required that less than 0.75 GeV was deposited.

Acknowledgements. We gratefully acknowledge the support of the DESY directorate, the PETRA machine group for high luminosity running and the staff of the DESY computer centre. Those of us from outside DESY wish to thank the DESY directorate for the hospitality extended to us.

References

1. S.L. Glashow: Nucl. Phys. 22 (1961) 579; Rev. Mod. Phys. 52 (1980) 539; A. Salam: Phys. Rev. 127 (1962) 331; Rev. Mod. Phys. 52 (1980) 525; S. Weinberg: Phys. Rev. Lett. 19 (1967) 1264; Rev. Mod. Phys. 52 (1980) 515
2. TASSO Coll. R. Brandelik et al.: Phys. Lett. 110B (1982) 173; TASSO Coll. M. Althoff et al.: Z. Phys. C – Particles and Fields 22 (1984) 13
3. C.M. Hawkes: D. Phil Thesis, Oxford University, RAL T 011 (1985)
4. C. Balkwill: D. Phil Thesis, Oxford University, in preparation (1988)
5. TASSO Coll. W. Braunschweig et al.: Z. Phys. C – Particles and Fields 37 (1988) 171
6. F.A. Berends, R. Kleiss, S. Jadach: Nucl. Phys. B 202 (1982) 63
7. R.J. Cashmore et al.: Z. Phys. C – Particles and Fields 30 (1986) 125
8. M. Böhm, W. Hollik: Phys. Lett 139 B (1984) 213
9. B. Lynn, R. Stuart: Nucl. Phys. B 253 (1985) 216
10. I. Brock: D. Phil Thesis, Oxford University, RL-HEP/T/106 (1983)
11. A. Böhm: Proc. xiv ème Rencontre de Moriond (1984) Vol. 1, p 191
12. Particle Data Group: Review of Particle Properties, Phys. Lett 170 B (1986); UA2 Coll. R. Ansari et al.: Phys. Lett. 186 B (1987) 440; UA1 Coll. G. Arnison et al.: Phys. Lett. 166 B (1985) 484
13. U. Amaldi et al.: Phys. Rev. D 36 (1987) 1385
14. E.J. Eichten, K.D. Lane, M.E. Peskin: Phys. Rev. Lett. 50 (1983) 811
15. CELLO Coll. H.-J. Behrend et al.: Z. Phys. C – Particles and Fields 14 (1982) 283; Phys. Lett. 191 B (1987) 209, and contribution to the 1987 Int. Symp. on Lepton and Photon Interactions, Hamburg,
    JADE Coll. W. Bartel et al.: Z. Phys. C – Particles and Fields 26 (1985) 507; B. Naroska: Phys. Rep. 148 (1987) 67; and contribution to the 1987 Int. Symp. on Lepton and Photon Interactions, Hamburg;
    Mark J. Coll. B. Adeva et al.: Phys. Rev. Lett 55 (1985) 665; J. Mnich: Thesis, RWTH Aachen, 1987;
    PLUTO Coll. Ch. Berger et al.: Z. Phys. C – Particles and Fields 27 (1985) 341